ANALYSIS OF PALAEOMAGNETIC TIME SERIES – TECHNIQUES AND APPLICATIONS

CHARLES E. BARTON

Graduate School of Oceanography, University of Rhode Island, Kingston, RI 02882 U.S.A.

Abstract. This review is intended to provide an introduction for the nonspecialist to concepts and techniques which are useful for analysing palaeomagnetic time series. Emphasis is placed on analysis in the frequency domain, particularly the periodogram and maximum entropy methods. The review consists of two parts dealing with techniques and applications respectively.

1. Techniques

1.1. INTRODUCTION

The complexities of both source mechanisms and the recording process through which we see the geomagnetic field are such that no two secular variation records stemming from the same source would be identical. At every time, t, we can associate a set of probabilities with the occurrence of each of the possible values $X(t)$ of the time dependent variable. This set of random variables and associated probability distributions is called a stochastic process. The time series we observe is treated as a sample of one of the infinite set of realisations of the process (Figure

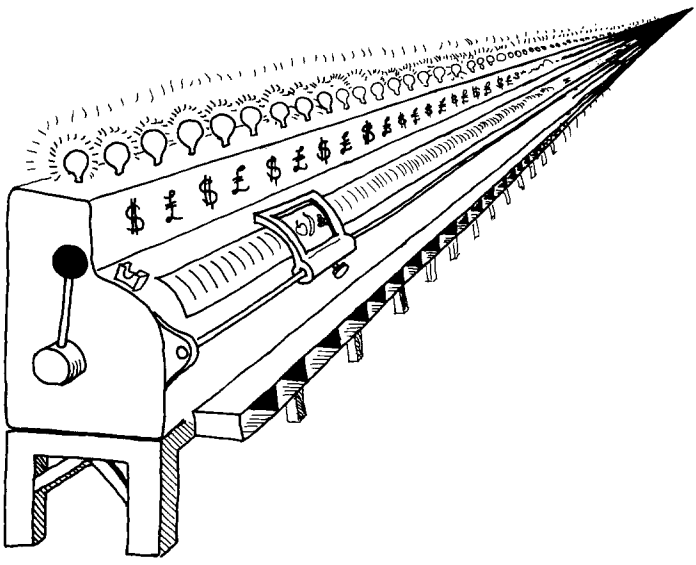

Fig. 1. A stochastic process in operation.

Geophysical Surveys **5** (1983) 335-368. 0046–5763/83/0054-0335$05.10.

1). The object of time series analysis is to estimate the properties and parameters governing the stochastic process from the limited information contained in the observed finite record. The consequences of the inherent assumptions in doing this become particularly acute for records which are short compared with the periods of interest. Fourier transform based spectral estimates (periodogram and auto-variance) require strong assumptions about the data outside the observed record. This is less true of recent non-linear parametric modelling techniques (e.g. the maximum entropy method, MEM) which are gaining rapid acceptance due to their potentially superior resolution and ability to cope with short series.

Introductions to the concept of the power spectrum of a process, and the spectral density function are to be found in any reference texts on time series analysis. Chatfield (1980) gives a particularly straight-forward account. The power spectrum is a line spectrum which expresses the variance (power) of the time series in terms of the variances of a set of components at discrete frequencies into which the series can be decomposed. In practice the decomposition can only be performed approximately and requires assumptions about the nature of the series outside the observed range. The variance assigned to each of the discrete frequencies will be a function of how many frequencies are used within a given band. The limiting case of a continuous frequency distribution is best described by the power spectral density function, $S(f)$, which is a continuous function of frequency. The variance of the process accounted for by frequencies in the range f_1 to f_2 is given by:

$$\text{Variance} = \int_{f_1}^{f_2} S(f)\ \mathrm{d}f$$

i.e. by the area beneath the curve (Figure 2). The power spectrum and the spectral density functions are fundamentally different even though an estimate of the latter can easily be obtained from the former (see below). For example, $S(f)$ is undefined for a pure harmonic at frequency f, since this would require a finite area beneath the curve for an infinitessimal bandwidth.

The ensuing discussion assumes that the statistical properties of the times series do not vary with time, i.e. that the stochastic process is stationary, and also that

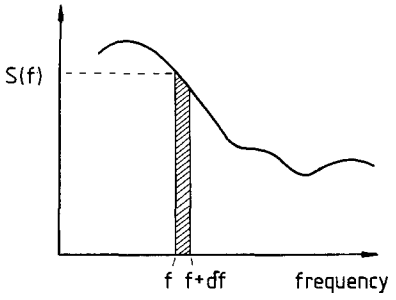

Fig. 2. Spectral power density, $S(f)$, as a continuous function of frequency. Variance accounted for by frequencies in the small interval f to $f+\partial f$ is $S(f)\partial f$, i.e. the shaded area beneath the curve. The concept may be extended to finite intervals by simple integration.

points are spaced at equal time intervals (Δt). This limits the highest detectable frequency in the data to $1/2\Delta t$ which is called the Nyquist cutoff frequency (f_c).

1.2. PERIODOGRAM (DET) METHOD

The discrete Fourier transform (DFT) approach to finding hidden periodicities was suggested by Schuster (1978). The squared amplitude of the transform was used as the spectral estimate. In practical terms the method is equivalent to using a least squares technique to fit a sequence of sinusoids to the data, whose periods are integer divisors of the length of the record. The series is thus decomposed into a set of harmonics.

To simplify the notation, consider a time series x_t, $t = 0, 1 \ldots, N-1$ with an odd number of terms (N) equally spaced at interval Δt, and with zero mean. A discrete Fourier transform of the series gives the cosine and sine transforms, A_j and B_j, at each of the Fourier angular frequencies $w_j = 2\pi j/N\Delta t, j = 1, 2 \ldots (N-1)/2$ where

$$\left.\begin{aligned} x_t &= \sum_j [A_j \cos(w_j t) + B_j \sin(w_j t)] \\ \text{and} \quad A_j &= \frac{2}{N}\sum_t x_t \cos(w_j t); \quad B_j = \frac{2}{N}\sum_t x_t \sin(w_j t) \end{aligned}\right\} \tag{1}$$

A_j and B_j are least-squares estimates of the amplitudes of the best fitting cosine and sine waves at each frequency w_j. The amplitude and phase of the j^{th} harmonic are thus given by $R_j = (A_j^2 + B_j^2)^{1/2}$ and $\Phi_j = \tan^{-1}[-B_j/A_j]$, and the power (variance) accounted for by each harmonic is:

$$P_j = \frac{R_j^2}{2} .$$

The term power, rather than variance, derives from the electrical analogue: Power dissipated = rms current^2 × resistance = $\frac{1}{2}$ × peak current^2 × resistance. The total variance is the sum of the variances accounted for by each harmonic (Parseval's theorem). The amplitude and power spectrum are plots of R_j and P_j against frequency respectively. The case of $j = 0$ may be ignored since the mean of the series $A_0/2$ is zero. The Nyquist frequency $f_c = 1/2\Delta t$, or $w_c = \pi/\Delta t$, hence the upper limit for j in (1) is (N–1)/2.

It is notationally and compuationally convenient to express (1) in complex number form using the Euler relation,

$$\cos wt + i \sin wt = \exp(-iwt)$$

namely,

$$\left.\begin{aligned} x_t &= \sum_{j=1}^{N-1} J_j \exp(iw_j t) \\ J_j &= \frac{1}{N}\sum_{N-1}^{t_{N-1}} x_t \exp(-iw_j t) \end{aligned}\right\} \tag{2}$$

whence

$$J_j = \tfrac{1}{2}(A_j - iB_j). \tag{3}$$

The set of N complex numbers $J_0, J_1 \ldots J_{N-1}$ is the Fourier transform of x_t. J_0 is zero since the mean of x_t is zero. The squared modulus of the transform

$$|J_j|^2 = J_j J_j^* = \tfrac{1}{4}(A_j^2 + B_j^2) = \tfrac{1}{4}R_j^2 = \tfrac{1}{2}P_j^2,$$

where * denotes the complex conjugate.

The periodogram function, $I(w)$, is a power spectral density estimate. If we treat the power at w_j as distributed over a frequency interval equal to the spacing of the Fourier angular frequencies, $\Delta w = 2\pi/N\Delta t$, then power within $w_j \pm \frac{1}{2}\Delta w$ = area beneath the spectral density curve i.e. $R_j^2/2 = I(w_j)\Delta w$, hence, $I(w_j) = N\Delta t/4\pi \times R_j^2$. In terms of frequency, the spacing is $\Delta f = 1/N\Delta t$, and

$$I(f_j) = \frac{N\Delta t}{2} R_j^2. \tag{4}$$

We have only considered positive frequencies, so (4) is an estimate of the 'one-sided' spectral density. A more systematic approach, which allows for complex as well as real data, is to equate the total variance to the area beneath the spectral density curve within the frequency range $-f_c \leq f < f_c$. The periodogram estimate for the 'two-sided' spectral density function becomes $(N\Delta t/4)R_j^2$.

The significance and interpretation of negative frequencies is discussed in Section 1.5.

The periodogram method initially fell out of favour due to (i) problems in interpreting the periodogram which can behave erratically and look remarkably different for time series with similar characteristics (Jenkins and Watts, 1968, Chapter 6, Bloomfield, 1976), and (ii) the large number of computations involved in calculating the Fourier transform of long time series. The advent of the fast Fourier transform routine (Cooley and Tukey, 1975) which reduces the number of multiplications and additions from $\sim N^2$ to $\sim N \ln N$, combined with the knowledge that smoothing of the periodogram, using suitably weighted averages of adjacent ordinates, leads to a stable spectral estimate, have combined to re-establish the popularity of the method (Jones, 1965).

The spectrum obtained is actually that of the infinite time series composed of periodic repetitions of the observed data, i.e. a periodic extension of the data is assumed. Poor resolution at the low frequency end of the spectrum is unavoidable since the periodogram is only computed for periods equal to $\frac{1}{j}$ times the record length. Repeated analysis of different sections of the full record provides a means of identifying those features of the periodogram which are statistically invariant with time and therefore represent the 'spectrum' of the stochastic process. By extending the length of the record with zeros the frequency spacing can be artificially reduced. The usefulness of both these approaches is limited by the underlying periodic assumption which means that periodograms based on altered versions of the observed record apply to different infinite time series. The object of smoothing

periodograms in the frequency domain is to obtain a stable spectral estimate without resorting to the above techniques. Kane (1977) has compared unsmoothed periodograms for real and synthetic harmonic data with composites derived from analyses of a range of truncations of the original series. His results demonstrate that this superposition method can give improved resolution and better frequency fidelity in the high frequency region of the spectrum ($j \geqslant 6$), where the results are 'comparable to, and in some respects superior to, Burg's method of maximum entropy'. Smoothing of the periodogram does not change this conclusion substantially. Recent experiments with truncated real sinusoids (Swingler, 1980) have shown that even for short record lengths the discrete Fourier transform may be superior to the maximum entropy method as a frequency estimator, depending on the initial phase and the number of cycles within the record length at a given frequency. This is discussed further in Section 1.4.

1.3. THE AUTOCOVARIANCE METHOD

This method (Blackman and Tukey, 1959) was the most widely used spectral estimation scheme until the revival of the periodogram approach after 1965. The latter is now generally preferred for finite length records (Jones, 1965, Jenkins and Watts, 1968, p. 7), though recently evidence has been accumulating which favours the use of weighted covariance estimates (Koopmans, 1974, p. 325+).

The autocovariance of an N point series $x(t)$ at lag r is defined as

$$C_r = \frac{1}{N} \sum_{t=0}^{T-r} x(t+r)\ x(t),$$

where $T\ (=N\Delta t)$ is the length of the series. C_r can be thought of as the mean of the product of adjacent terms when the series is compared with itself displaced in time by lag, r. Provided certain basic conditions are met, the autocovariance function at lag r of the stationary stochastic process $Y(t)$ is given by

$$C_r = \lim_{T \to \infty} \frac{1}{T+1} \sum_{t=0}^{T} y(t+r)y(t)^*$$

and the spectral density function can be shown to be the Fourier transform of the autovariance:

$$S(w) = \frac{1}{2\pi} \sum_{r=-\infty}^{\infty} C_r \exp(-irwt). \tag{5}$$

In the above, $y(t)$ is an infinite set representing one realisation of the process $Y(t)$. If $y(t)$ is equated to the observed time series over the length of the record, and made zero elsewhere, then an estimate of the autocovariance function is

$$\hat{C}_r = \frac{1}{T+1} \sum_{t=0}^{T-r} y(t+r)\ y(t)^*,$$

where $t=0$, T is the range of the finite data. This is used to compute the spectrum from Equation (5). The null extension of the data is a strong assumption and can lead to large errors unless the length of the series is many times the longest period of interest. The method is computationally economical.

In practice, a stable estimate of $S(w)$ is obtained by truncating the summation, at lag $r = M$ say, and by weighting the autocovariances:

$$\hat{S}(w) = \frac{1}{2\pi} \sum_{r=1}^{M} h_r C_r \exp(-iwr).$$

The set of coefficients, h_r (the lag window), is chosen to reduce the effect of autocovariances at large lags. There is an extensive literature covering the merits of various lag windows and truncation points. Two of the most commonly used are the Tukey (or Blackman-Tukey) window:

$$h_r = \frac{1}{2}\left(1 + \cos\frac{\pi r}{M}\right) r = 0, 1, \ldots, M$$

and the Parzen window:

$$h_r = \begin{cases} 1 - 6\left(\frac{r}{M}\right)^2 + 6\left(\frac{r}{M}\right)^3 & 0 \leq r \leq M/2 \\ 2\left(1 - \frac{r}{M}\right)^3 & \frac{M}{2} \leq r \leq M. \end{cases}$$

An efficient procedure for computing the Tukey window, named after Julius Von Hann, is called 'Hanning'. 'Hamming' is a minor variant of this using slightly different weights, named after R. W. Hamming.

In fact, the periodogram and autocovariance approaches are essentially equivalent, apart from differences in windowing and smoothing, since it follows that:

$$I(w_j) = \frac{1}{\pi}\left[C_0 + 2 \sum_{r=1}^{N-1} C_r \exp(-iw_j r)\right].$$

The factor $1/\pi$ is replaced by $1/2\pi$ in the equivalent expression for the two-sided estimate.

1.4. THE MAXIUM ENTROPY METHOD

The above two methods see the data through a pre-selected, fixed window and require the unrealistic assumption of a periodic or a null extension outside the observed record. Hence the possibility of poor resolution and shifts in the spectral peaks when the methods are applied to 'short' data sequences (Toman, 1965). It is intrinsic in some of the newer parametric modelling approached that the data window is generated from the data itself, hence Lacoss's (1971) term 'data adaptive methods'. A fundamental parametric model is the discrete autoregressive (AR) process, proposed by Yule (1927). The value of the variable at time t, $X(t)$, is

derived linearly from a purely random Gaussian process according to the previous m values of the variable:

$$X(t) = a_1X(t-1) + a_2X(t-2) + \ldots + A_mX(t-m) + B(t), \tag{6}$$

where m is known as the order of the autoregressive process, $a_1, a_2, \ldots, a_m$ are constants, $B(t)$ is called the innovation of the process, and the mean of both the AR process and $B(t)$ are zero. The AR process may be viewed as a prediction of $X(t)$ from the previous m values of X, and $B(t)$ as the prediction error. It has been shown by many authors (e.g. Ulrych and Bishop, 1975) that the spectrum of the m^{th} order autoregressive process is

$$S(f) = 2\beta_m^2 \left| 1 - \sum_{j=1}^{m} a_j \exp(-i2\pi fj) \right|^{-2}, \tag{7}$$

where β_m is the variance of $B(t)$. $S(f)$ can be evaluated at all frequencies between $\pm f_c$.

The maximum entropy method of spectral analysis has become increasingly popular since its introduction by Burg (1967, 1968) and has been applied successfully to a variety of geomagnetic and geophysical problems. Of the many discussions of the method which have published, McGee (1969), Smylie *et al.* (1973, Andersen (1974), Ulrych and Bishop (1975) and Kanasewich (1975) are particularly useful as an introduction. Andersen gives a logic flow diagram for the Burg algorithm and Ulrych and Bishop give Fortran subroutines for computing the filter coefficients, estimates of the autocovariances and Akaike's final prediction error criterion (below). Essentially the method involves fitting an autoregressive model to the data based on the principle that the resultant spectral estimate should be based on all the information in the actual record and assume the least possible amount of information (hence the name maximum entropy) about the series outside the observed record. The condition for this happens to be satisfied by the m^{th} order autoregressive process (6). The set of coefficients $(1, -a_1, -a_2, \ldots, -a_m)$, or more commonly $(1, \gamma_1, \gamma_2, \ldots \gamma_{m)}$ where $\gamma_1 = -a_1$ etc., is called the prediction error filter since the prediction error, $B(t)$, is the convolution of this filter with the vector $X(t)$. The spectrum of the process is thus estimated by Equation (7) which in frequency terms is

$$S(f) = \frac{P_{m+1}}{f_c} \left| \sum_{j=0}^{m} \gamma_j \exp(-i2\pi fj\Delta t) \right|^{-2},$$

where $\gamma_0 = 1$, and P_{m+1} is a constant representing the power (variance) of the $(m+1)$ term prediction error series $B(t)$, i.e. the prediction error power. The evaluation of P_{m+1} and then $S(f)$ requires estimation of the $(m+1)$ prediction error coefficients.

Ulrych and Bishop (1975) give a description of the commonly used Yule-Walker estimates of these coefficients, together with a recursive equation and a Fortran subroutine for performing the computations. The estimates are based in turn on estimates of the autocovariances:

$$C_r = \frac{1}{N} \sum_{t=1}^{N-|r|} [x(t+r) - \bar{x}]\,[x(t) - \bar{x}],$$

where $\bar{x}$ is the mean of $x(t)$. The use of these estimates in place of the true autocovariances of the process implies that $x(t) = 0$ for $|t| > t_N$, which is inconsistent with the maximum entropy concept.

Burg's estimates of the coefficients are based on the additional condition that the mean of the prediction error powers, obtained by running the filter in the forward and reverse direction over (but not off) the data, should be a minimum. The estimates are thus based on the observed data and make no rigid *a priori* assumptions about values outside this range. Prior estimation of the autocovariances of the process is not required, although they can easily be obtained from the prediction error coefficients both within the range of lags covered by the data and by extrapolation outside that range based on the maximum entropy principle (Ulrych and Bishop, 1975).

The remaining problem is the optimum selection of the order of the process. If m is chosen too low the spectrum is over-smoothed and the high resolution potential is lost. If m is chosen too high, frequency shifting and spontaneous splitting of the spectral peaks occurs (Fougere *et al.*, 1976), giving a false, peaky appearance to the spectrum. Objective methods for selecting m have been suggested by Akaike (1969a, b, 1970), Akaike (1974, 1976), Ulrych and Bishop (1975), Ulrych and Clayton (1976), Treitel *et al.* (1977), Berkhout and Zaanen (1976), and Berryman (1978) – also see Haykin (1979).

Since each is justified empirically, the current lack of a consensus is evidence that the best choice of criterion depends on the characteristics and length (N) of the data set in question. Furthermore, it appears that the value of m which leads to the most accurate frequency determination is itself a function of frequency (see for example Kane, 1977). A useful approach is that adopted by Jin and Thomas (1977) who plot the periods of the main spectral peaks as a function of m. Such diagrams clearly delineate the zones of instability, stability and line splitting, and also demonstrate how the region of stability varies with both m and frequency.

The most commonly used criteria are (i) Akaike's final prediction error, FPE (Akaike, 1969, 1970), (ii) Ulrych and Clayton's (1976) criterion: $m_{UC} = N/3$ to $N/2$, which the authors claim gives consistent results for short realisations of harmonic processes, and (iii) Berryman's criterion: $m_B = 2N\ (\ln 2N)^{-1}$, which he tests on decaying seismic signals. Akaike's final prediction error is estimated by

$$\hat{\text{FPE}} = \left[\frac{N+m+1}{N-m-1}\right] \beta_m^2,$$

where β_m^2 is the sum of the squares of the prediction errors after removing the mean from the data. The optimum value of m is that which minimises the above estimate. Ulrych and Bishop (1975) drew the following conclusions from their tests on short synthetic AR, autoregressive moving average (ARMA) and harmonic data sets (YW-FPE and BG-FPE denote FPE's based on the Yule-Walker and Burg auto-

covariance estimates respectively): (i) the variance of the YW-FPE is always less than the BG-FPE for any order, hence is generally preferred for applying the Akaike criterion, though far higher resolution spectrum is obtained by the Burg estimates, (ii) a cut off at approximately $m = N/2$ must be imposed when locating the minimum FPE based on the Burg scheme, (iii) the YW-FPE criterion underestimates the order of high order AR processes and harmonic processes, particularly the latter, (iv) the BG-FPE criterion gives generally correct results for AR series but tends to overestimate the order of ARMA processes, (v) in such cases, the first minimum of the BG-FPE gives more consistent results, but will severely underestimate the order of more nearly periodic data. Other authors who have tested the method are listed by Ulrych and Clayton (1976). For many data sets the criterion has been found inconclusive as the FPE fails to show a clearly defined minimum.

The problem of frequency shifts in the spectral peaks for short data sets is not eliminated by use of the MEM as shown by Chen and Stegen (1974) for sinusoidal data. They show that, depending on its initial phase, a sinusoid sampled at 1/20 cycle intervals can have its spectral peak shifted by up to about 100% for record length $L \simeq \frac{1}{4}$ cycle, 30% for $L \simeq \frac{3}{4}$ cycle, 12% for $L \simeq 1\frac{3}{4}$ cycles, 9% for $L \simeq 1\frac{3}{4}$ cycles, and 5% for $L \simeq 2\frac{3}{4}$ cycle. Frequency shifting does not occur for $L = k/2$ cycles for integer values of k for all initial phases. They conclude that provided the record spans more than a full cycle, a substantial range in length of the filter will yield a reeasonably good spectrum. Particularly for noisy data it is better to over-estimate rather than underestimate the order, and by increasing the density of data points a higher noise level can be tolerated before the spectrum becomes implausible. In his comparison of errors in estimating frequencies by the MEM and DFT method, Swingler (1980) points out that the latter exhibits zero error irrespective of initial phase if $L = (2k+1)/4$ cycles, and also that the DFT error drops off as N^{-2}, whereas the MEM error drops off more slowly, as $(N-1)^{-1}$. He concludes that 'even for modest data lengths (which depend on the frequency of interest but are typically perhaps 20 or so) the DFT may be regarded as superior as a frequency estimator for a truncated real sinusoid'.

It has been pointed out by Lacoss (1971) and others that the function $S(f)$ in Equation (7) corresponds to a power spectral density estimate. The integrated spectrum (area beneath the curve $S(f)$ vs f will be somewhat smoother and is the MEM analog of the power spectrum of the periodogram method. Only a few authors (e.g. Radoski *et al.*, 1975) actually perform the integration. The resulting power estimates will depend on the selected order of the AR model, which affects the width and amplitude of spectral peaks.

In view of the lack of objectivity in choosing m, the problem of frequency shifting, and the difficulty of obtaining quantitative power estimates it is obviously unwise to employ Burg's MEM without first performing a DFT analysis.

More sophisticated parametric models of particular relevance to the analysis of short harmonic series are Pizarenko's (1972) covariance matrix method, Ulrych and Clayton's (1976) least squares estimator, and Swingler's (1979) bi-directional

non-recursive method. The authors show that for truncated harmonic processes these methods give more accurate frequency determination than Burg's MEM (see also Swingler, 1980). The attraction of Burg's MEM is its computational simplicity and the large variety of data sets on which it has been tested.

A concise statement of Burg's algorithm for applying the MEM to complex data is given by Denham (1975) and a derivation of the equations used is in Smylie *et al.* (1973). A Fortran subroutine SMYLIE which implements Smylie's scheme is given in the Appendix. Subroutine SPECT computes the spectral density estimate, $S(f)$, from the filter coefficients for real data computed from, say, the subroutines YWPR or MEMPR (for the Yule-Walker or Burg estimates respectively) listed by Ulrych and Bishop (1975). Subroutine ANDS, based on Anderson's (1974) flow diagram, generates the PEF coefficients.

1.5. Frequency Spectrum of Complex Data and Vector Time Series

The DFT Equations (2) encompass negative as well as positive frequencies provided the $-j^{\text{th}}$ Fourier frequency is interpreted as

$$w_{-j} = \frac{2\pi(-j)}{N\Delta t} = -w_j$$

and we define $J_{-j} = J_j^*$.

Equations (4) still apply except that the range of j becomes $-N/2 < j < N/2$, and the mean square signal (average power) is

$$\sum |J_j|^2 = |J_0|^2 + \sum_{j>-N/2}^{1} |J_j|^2 + \sum_{j=1}^{<N/2} |J_j|^2$$

i.e. the sum of the contributions from the positive and negative frequency sides of the spectrum ($J_0 = 0$ since the series has zero mean). From Equations (1) and (3) it follows that for a real valued time series, A_j and B_j are real, so $|J_{-j}|^2 = |J_j|^2$ and the spectrum has positive symmetry about zero frequency.

For a complex valued series, $z(t) = x(t) + iy(t)$, the power density, $S(f)$, in the positive and negative halves of the spectrum at frequency f will generally be unequal. It can easily be shown that the vector $z(t)$ describes a clockwise circle in the complex plane at a given frequency if $S(f) = 0$ and $S(-f) > 0$, an anticlockwise circle for the converse situation, and no rotation if $S(f) = S(-f)$. The general case, $S(f) \neq S(-f) \neq 0$, corresponds to elliptical motion in the sense determined by the power bias.

Two-dimensional vector time series can thus be analysed as a single complex number series with real and imaginary parts equal to the Cartesian co-ordinates of the vector. This approach has been elaborated by Gonella (1972) in his analysis of wind and ocean current data and has been used by Brillinger (1973) to analyse the Chandler wobble. Gonella defines a *rotary coefficient* at frequency $\pm w_j$:

$$C_{Rj} = \frac{|J_{-j}|^2 - |J_{+j}|^2}{|J_{-j}|^2 + |J_{+j}|^2}$$

which varies between + 1 for pure clockwise rotation and – 1 for pure anticlockwise rotation, and is zero for unidirectional motion. It is invariant under co-ordinate transformation or scaling of the spectrum, and provides an objective means of quantifying the rotation associated with the asymmetry of the spectrum.

Denham (1975) demonstrated how the method can be applied to palaeomagnetic data: directions are centred about a suitable norm (e.g. axial dipole field direction or the vector mean of the data) and projected on to a plane surface using some spherical projection to generate Cartesian coordinates, which are treated as the real and imaginary parts of the complex number series. For widely dispersed directions, projection on to a plane introduces considerable distortion which will be manifested at the high frequency end of the spectrum. Denham gives mapping functions for the common projections normalized to give equal projected radii at angle 45° from the pole. A better compromise for producing less average distortion for directions with low scatter, e.g. most smoothed secular variation records, is to equalize radii at angle = 20° (Table I).

TABLE I

Mapping functions of the common spherical projections for equal projected radius at polar angle $\theta = 20°$

Projection	Projected radius
Equidistant	2.865 θ (in radians)
Gnomonic	2.747 tan θ
Orthographic	2.924 sin θ
Stereographic	5.671 tan (θ/2)
Lambert equal area	5.749 sin (θ/2)

Little has been done to test the maximum entropy method on complex number series. Barton and McElhinny (1982) examined a data set synthesized from a Gaussian random noise component added to a signal generated at 40° N by a virtual geomagnetic pole precessing at 70° N. They concluded: (i) for a given order of the AR model, m, the spectra of vector equivalent complex series are much smoother than their counterparts for independent declination or inclination series, (ii) power is confined to the appropriate side of the spectrum for a suitable range of m, (iii) if the order is underestimated peaks are shifted to lower frequency, and (iv) if the order is over estimated, a power bias on the wrong side of the spectrum may occur and the spectrum becomes unstable with respect to change of order. Tests on a similar series with zero rotational component indicated that the MEM spectrum is even smoother for a given order, and (for short noise-free realisations) the spectrum is sensitive to the choice of m. These observations demonstrate that care must be taken in the choice of m, and that the objective criteria for real data underestimate m for complex data.

An alternative to the complex number approach to analysing vector time series for rotary components is provided by cross-spectrum analysis. Two series are compared in the frequency domain to determine the level of coherence (for 0 to 1) and the phase difference between harmonics of each series at a given frequency (see for example Bloomfield, 1976, Chapter 9). If this is done for declination and inclination series, it follows that a high level of coherence coinciding with a phase difference of $\sim \pm \pi/2$ at a particular frequency implies clockwise or anticlockwise precession of the magnetic vector, depending on the sign of the phase difference. Phase differences of 0 or π correspond to the case of non-rotation. However, the method has a poor resolution compared with the complex number approach and is less easy to interpret.

1.6. PRACTICAL CONSIDERATIONS

Analytical methods discussed above assume equal time intervals (t) between data points. There are methods which do not require this constraint (e.g. Deeming, 1975), but these are seldom warranted for palaeomagnetic time series. Variance associated with frequencies higher than the Nyquist is not lost, but appears added to (aliased with) powers in the range $-f_c$ to $+f_c$, thus distorting the estimated spectrum. Lacustrine sedimentation rates are typically $\sim 50\,\text{cm Kyr}^{-1}$, hence for cores subsampled at 2.5 cm intervals, the Nyquist period is ~ 100 yr. This figure is also representative of most of our best archaeomagnetic records. Since physical and chemical constraints intrinsically cause averaging which generally limits the resolution of palaeomagnetic records and radiocarbon chronologies to below this level, aliasing problems are seldom important in practice. For scattered data, such as palaeomagnetic time series, equi-spacing is generally achieved by some form of smoothing and interpolation. One of the simplest forms of smoothing is to take moving averages, and then do a linear interpolation to obtain a series of equi-spaced points. A variant of this is to shift the averaging window at equal time intervals (hence the number of points averaged varies between steps).

Various 'robust' methods of smoothing exist which offer great stability even when applied to erratic data (e.g. Claerbout and Muir, 1973; Claerbout, 1976; Tukey, 1977; McNeil, 1977). Such methods are designed to overcome the problem of outliers, which bias moving averages, for example by using the median instead of the mean. Again, one of the simplest robust smoothing/interpolating methods is to take the median for consecutive equal intervals of time. A useful compromise is to use inter-quartile means (i.e. the mean after discarding upper and lower quartiles) instead of medians.

A different approach is to fit a smooth curve through the data prior to interpolation. This is particularly useful for small sets of data. Cubic spline methods (e.g. DeBoor, 1978) are one of the most successful. A set of points (knots) is chosen at intervals throughout the record length, then a cubic curve is fitted by the method of least squares to the data between each knot, using the additional constraints that

there should be no change in slope across knots. A degree of robustness can be built into the technique by weighting outliers. The interval between knots (which need not be constant) determines the level of smoothing. Clark (1975) and Clark and Thompson (1978) describe a data-adaptive (cross-validation) method of choosing the appropriate spacing and generating confidence intervals.

To comply with the stationarity assumption, it is common practice to subtract the mean value from the data prior to analysis. An alternative, and equally simple, method of detrending is to transform the series by taking first order differences (Box and Jenkins, 1970). e.g. $X(t) = X_1, X_2, X_3, X_4 \ldots X_N$ becomes $Y(t) = (X_2 - X_1)$, $(X_3 - X_2)$, $(X_4 - X_3)$, $\ldots$, $(X_N - X_{N-1})$. Second order differencing of $X(t)$ is the same as first order differencing of $Y(t)$, and so on. Other commonly used forms of detrend involve fitting linear, polynomial or exponential curves to the data and then computing residuals. Detrending is a powerful technique which supresses the zero and very low frequency power in the spectrum and can have a profound effect on the shape and scaling of spectral estimates. The effect of detrending on MEM spectra has received only scant attention in the literature (e.g. Jin and Thomas, 1977; Courtillot *et al.*, 1977).

The phenomenon of one frequency in the data causing the Fourier transform to be non-zero at other frequencies is known as side-lobe leakage (e.g. Jenkins and Watts, 1968, p. 282). As series are only analysed in terms of the Fourier frequencies (i.e. harmonics of the record length), which will not generally correspond to periodicities in the data, leakage is very common. Abrupt truncations of the data, such as occur at the start and end of the record, are the most serious sources of leakage. The most common method of reducing leakage is to smooth these discontinuities by applying a split cosine bell window to the whole record. A preselected fraction of the data at the beginning and end of the series is amplitude modulated by one quarter of a cosine wave. Resulting spectrum estimates must then be scaled to compensate (e.g. multiply by a factor of 1.143 for a 10% taper applied to each end, Bendat and Piersol, 1971, p. 323).

The simplest and most economical fast Fourier transform algorithms require that the number of data points be an integer power of 2 (e.g. Sande-Tukey algorithm, listed in Bloomfield, 1976, p. 75). In practice records are either truncated to satisfy this requirement, or extended (padded) with zeros to the next higher radix-2 number of points. If N_1 points are extended to N_2, estimates of the power spectrum should be corrected by multiplying by $(N_2/N_1)^2$. The best known algorithm for the case of general N is due to Singleton (1968). DeBoor (1980) gives a much more compact, though less efficient algorithm which is particularly useful for very small computers.

Smoothing of the periodogram to get an estimate of the spectrum was first suggested by Daniell (1946) and has since been developed by many authors. Bloomfield (1976) describes a modified discrete Daniell smoothing procedure, together with Fortran subroutines. The filter of half width k is a simple moving average applied to the periodogram with weights:

$$\frac{1}{2k}(0, \ldots, 0, \tfrac{1}{2}, 1, 1, \ldots, 1, \tfrac{1}{2}, 0, \ldots, 0),$$

where the number of non-zero weights is $(2k + 1)$. More complex filters are built up by repeated applications of simple filters. Figure 3 shows the result of smoothing a unit impulse by various combinations of Daniell filters. The choice of spectral window depends on the conflicting requirements of resolution, stability, leakage and smoothness of the resultant spectrum. In these respects the modified Daniell procedure has certain optimum properties (Bloomfield, 1976, p. 172).

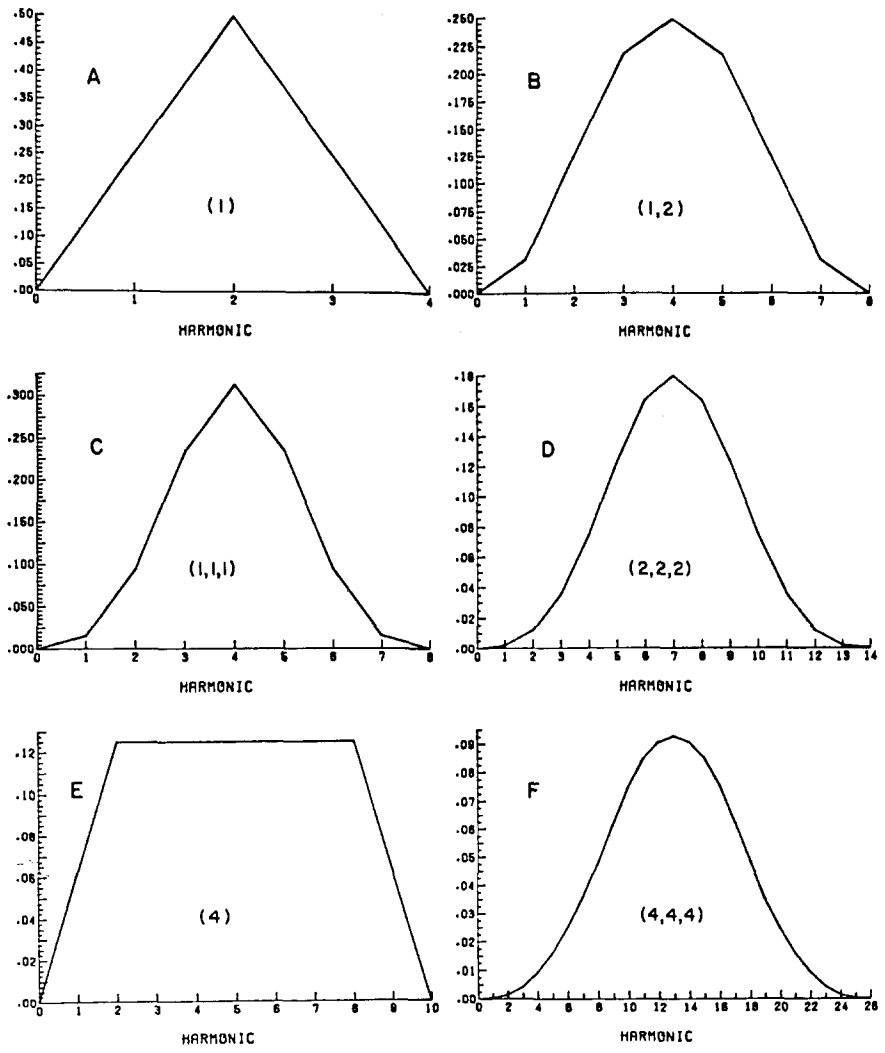

Fig. 3. Effects of smoothing a single line spectrum of unit height by various combinations of modified discrete Daniell filters. Numbers in brackets are half-widths of each successive application of the simple filter. All combinations have an equivalent single filter, e.g. the two passes (1, 1) are equivalent to a single pass of a filter with weights $\frac{1}{4}(0, \ldots, 0, \frac{1}{4}, 1, 1\frac{1}{2}, 1, \frac{1}{4}, 0, \ldots, 0)$.

1.7. REVERSAL SEQUENCES

Techniques for analysing 'analog' signals discussed so far are often inappropriate for binary signals such as the geomagnetic polarity sequence. Binary signals, or telegraphic waves, have a time dependent variable which can have one of only two values: normal (N or $+1$) and reversed (R or -1). Such sequences may be treated either as a set of alternating intervals (polarity states), or as a series of single point events (polarity transitions). In the latter case no distinction is made between N to R and R to N transitions. This can be overcome by treating the set of normal polarity intervals and the set of reversed polarity intervals as separate point processes (Phillips, 1977). Three possible ways of combining a periodic reversal signal with a noise component are listed by Phillips and Cox (1976). (Simple superposition of periodic and random binary waves, Figure 4a, results in a 3-state outpunt which is unacceptable): (i) Point processes can be superposed (Figure 4b) provided co-incident transitions are not allowed, (ii) the noise component may perturb the position of transitions in the periodic wave, and (iii) there could be a periodic modulation of interval lengths (i.e. the reversal frequency).

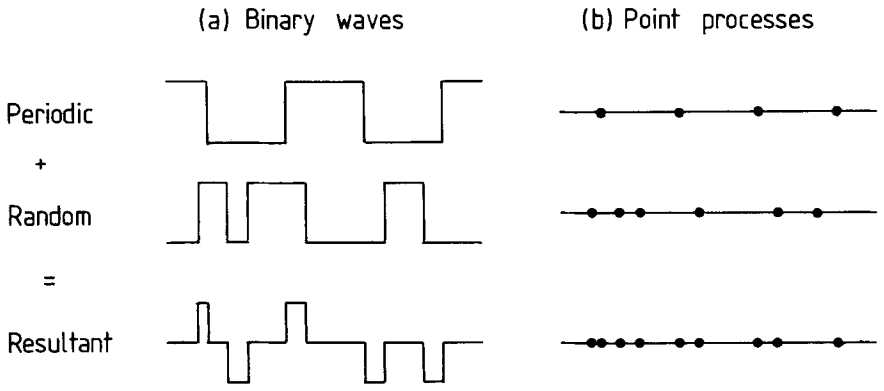

Fig. 4. (a) Superposition of a random binary wave on a periodic binary wave results in a 3-state wave. (b) Superposition of two point processes results in another point process which can be treated as a binary wave. Redrawn after Phillips and Cox (1976).

The most commonly used models are based on the general renewal process for which the probability of a transition occurring after elapsed time, t, since the previous transition is a function of t only. This means the process has no memory beyond the end of the previous transition. A useful extension of this model is the alternating reversal process in which probability distributions for N to R and R to N transitions are not the same (Phillips *et al.*, 1975). Particular classes of renewal process are characterized by the form of the distribution of intervals (T) between transitions. For example, for a gamma renewal process, T is a random variable from a gamma distribution with probability density function:

$$p\,df(T) = \frac{1}{\Gamma(k)}\left[\frac{k}{\mu}\right]^k T^{k-1}\exp\left(\frac{-kT}{\mu}\right)$$

(i.e. the probability of an interval of length between T and $T+dT$ is $p\,df(T)\,dT$, the area beneath the curve $p\,df(T)$ vs T). The gamma function is defined

$$\Gamma(k) = \int_{x=0}^{\infty} x^{k-1}\,e^{-x}\,dx$$

and may be evaluated from statistical tables. It follows that

$$\Gamma(k) = (k-1)\,\Gamma(k)-1)$$

and for positive integer values of k, $\Gamma(k) = (k-1)!$, and $\Gamma(1) = 1$. The average interval length and the variance of T are both equal to μ, and k is called the index of the distribution.

As $k \to \infty$, all interval lengths tend to a constant value, μ.

For $k >> 1$, the distribution is approximately Gaussain, i.e.

$$p\,df(T) = \frac{1}{\sigma\sqrt{2\pi}}\exp\left[\frac{-(T-\mu)^2}{2\sigma^2}\right]$$

with mean μ, and standard deviation σ.

For $k > 1$, the distribution peaks away from the origin.

For $k = 1$ we have the special case of a Poisson process,

$$p\,df(T) = \frac{1}{\mu}\exp\left[-\frac{T}{\mu}\right]$$

i.e. intervals are exponentially distributed with mean and variance, μ, The average number of transitions per unit time is therefore $1/\mu$, and the probability of a transition after elapsed time, t, since the last transition is constant. Poisson distributions arise naturally in situations involving the overall success of a large number of trials, each with a small probability of success.

The justification for assuming that core processes have no memory beyond the previous transition comes from the contrast between typical polarity intervals (0.33 My) and the inferred characteristic times of fluctuations in the non-dipole and dipole fields ($\lesssim 10^4$ yr). If, in fact, the probability of a transition $p(t)$ depends on the history of the process prior to the previous transition, then a 2-state Markov process model is appropriate (e.g. Cox and Miller, 1975). The Poisson process may be thought of as a special case of a Markov process.

To investigate periodic characteristics of polarity reversals it is convenient to turn to the frequency domain. For a random square wave from a Poisson process with amplitude A and average transition frequency f_0, the spectral density function is (Lowes, personal communication):

$$S(f) = \frac{4A^2}{f_0}\left[1+\left(2\pi\,\frac{f}{f_0}\right)^2\right]^{-1}.$$

If, say $A = 45000$ nT and $f_0 = 3$ reversals per 10^6 yr,

$$\text{for } f << f_0,\ S(f) \simeq \frac{4A^2}{f_0} = 2.7 \times 10^{15}\ \text{nT}^2\ \text{yr}.$$

$$\text{for } f > f_0,\ S(f) \simeq \pi^2 A^2 f_0 \frac{1}{f^2} = 6 \times 10^4 \frac{1}{f^2}\ \text{nT}^2\ \text{yr}.$$

Thus as frequency increases there is an inverse square law decay in power density from a peak value of about 3×10^{15} nT^2 yr.

Spectral analysis techniques for binary time series are described by Lee (1960). Phillips and Cox (1976) applied both Fourier analysis and maximum entropy techniques to the reversal time scale, and derived expressions for the theoretical spectrum for both semi-periodic and gamma renewal processes. Laj *et al.* (1979) discuss the properties of the autocorrelation function in the context of polarity time sequences.

2. Applications

2.1. Introduction

Palaeomagnetic time series arise from: (i) direct observation of the field elements, (ii) records of the geomagnetic secular variation obtained from archaeomagnetic measurements on baked clays, lacustrine and rapidly deposited marine sediments, (iii) the magnetic polarity time scale, and (iv) fluctuations in polarity bias and in the frequency of magnetic reversals. These classes are distinguished by very different time scales and recording processes (Figure 5).

Spectral analysis of palaeomagnetic time series has been largely restricted to the search for periodicities in the secular variation (Yukutake, 1962). The expectation of such studies is that characteristic periodicities in the nondipole and dipole fields exist, either because of intrinsic periodicities in source mechanisms, or because of uniform drift of sources relative to the Earth's crust. Other applications of time series analysis which have received less attention are (i) delineation of the continuous geomagnetic power spectrum, (ii) analysis of Bauer plots using complex number series, (iii) modelling source mechanisms by comparing declination, inclination and complex equivalent vector time series, and (iv) analysis of the reversal polarity time scale and variations in the polarity bias and frequency of reversals over geologic time. Comparisons of the power spectra of different phenomena can be used to infer common causal relationships.

Unfortunately, most of our information about the geomagnetic field in the past is directional only. There are few archaeointensity data prior to 10000 yr B.P., and only for the last few thousand years is there even an approximately global distribution of data (Barton, Merrill and Barbetti 1979). Fifteen years ago, a well defined sinusoidal variation in dipole moment during the last 10000 years with a period of

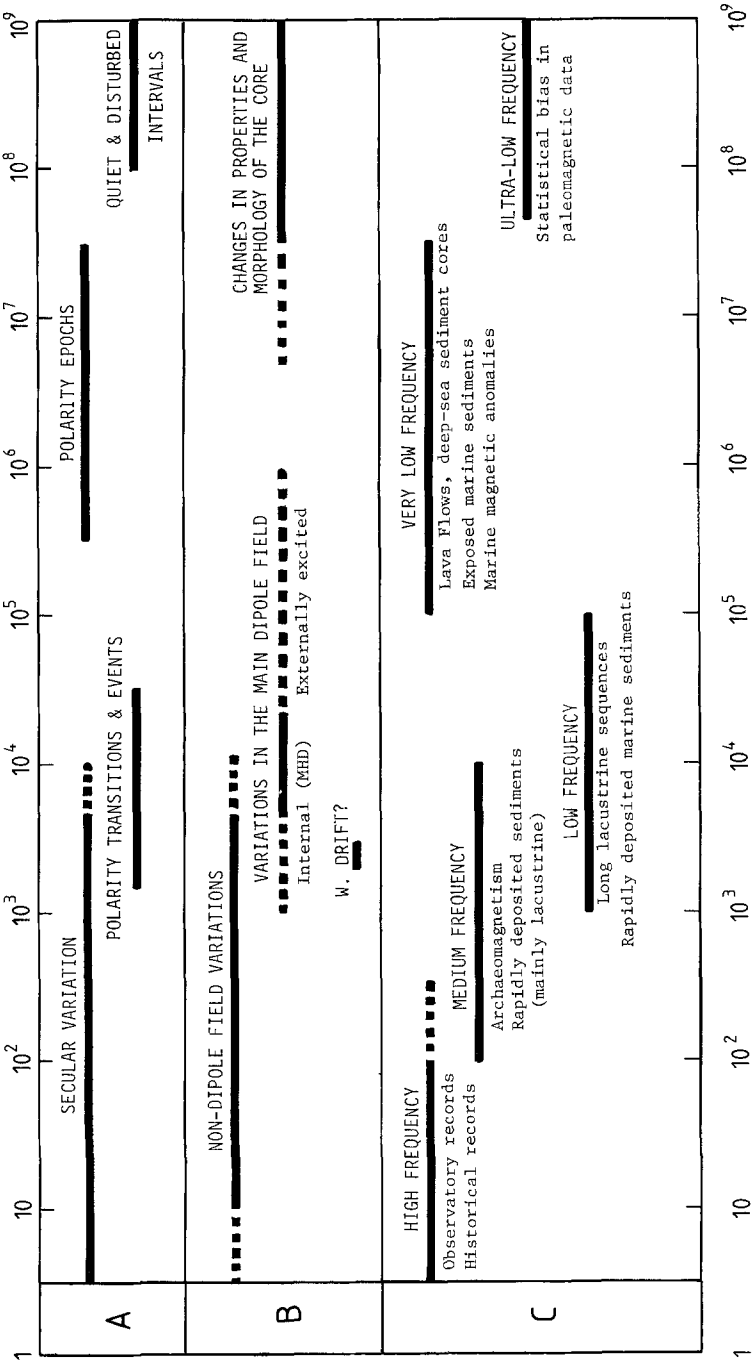

Fig. 5. Principal frequency bands of the geomagnetic spectrum of internal origin – their manifestation (A), possible origin (B), and mode of observation (C). Dividing lines between frequency bands are only intended to be approximate. The cutoff between the domains of internal and external sources occurs at about 13 yr (Alldredge 1977). Figure reproduced from Barton (1982).

about 8000 yr was reported (Bucha 1967, 1969; Cox 1968). A more complete data set demonstrates that this is largely a result of the dominance of European data (Barton, Merrill and Barbetti, 1979).

Analytical techniques and their limitations are discussed in Section 1. The dangers of misusing spectrum analysis are legion (Figure 6), particularly for parametric modelling methods (such as maximum entropy, MEM) for which the resulting spectrum is often sensitive to the largely subjective choice of model parameters. In the frequency domain we are estimating the time–invariant statistical properties of an infinite series of which the observed record forms a part. If the properties of geomagnetic signals vary with time (e.g. discontinuous phase shifts, or variations in frequency content occur), inferences drawn from the spectrum of the signal will be misleading.

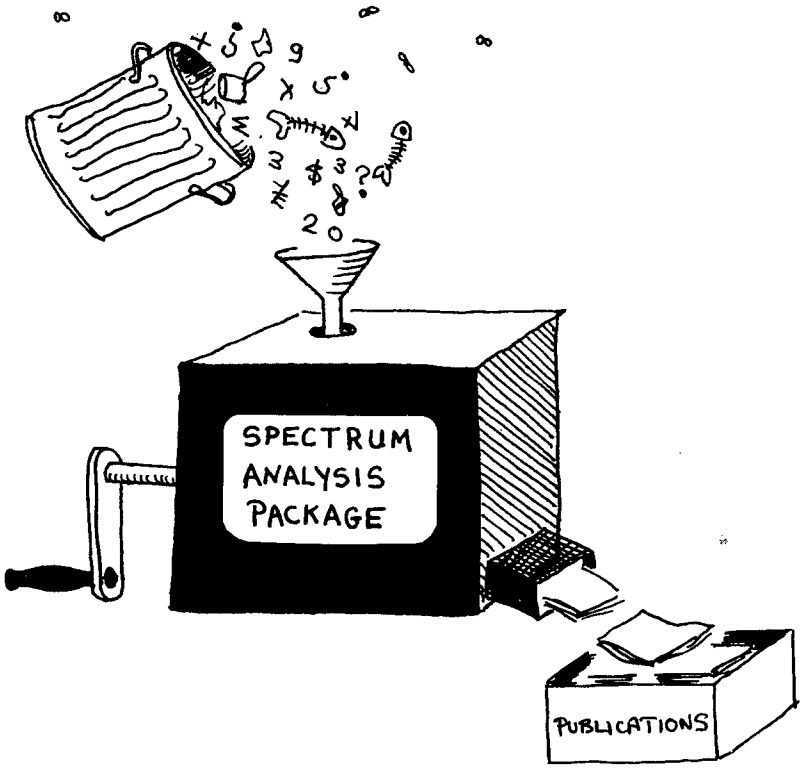

Fig. 6. A fail-safe analytical technique.

2.2. THE SEARCH FOR PERIODICITIES

Much effort has gone into trying to identify periodic components in the secular variation, both for describing dynamic processes in the core as well as for creating a basis for magnetic dating (Mackereth, 1971; Creer *et al.* 1972; Thompson and Turner, 1979; Stuiver, 1978). Records obtained from sediments particularly lake deposits, generally yield a continuous time sequence and are thus well suited for spectrum analysis.

The discovery of westward drift of the nondipole field with a period of about 2000 years (Bullard *et al.*, 1950), a sinusoidal variation in virtual dipole moments (Bucha, 1967, 1969; Cox, 1968), and regular swings in declination in lacustrine records (Mackereth, 1971) initially provided strong evidence for discrete periodicities in the geomagnetic signal. However, the acquisition of far more data during the last decade has failed to lead to a clear picture of what particular periods are characteristic of geomagnetic sources. The quality of most time scales are deplorable, and few authors have taken adequate steps to place uncertainty bounds on their spectral estimates. Nevertheless, we must conclude that discrete periodicities are not a world-wide feature of the secular variation. However, analyses of results from around the globe show a tendency for periodicities to fall into the following bands: 60–70, 400–600, 1000–3000, and 5000–8000 yr. The latter two bands are often, though not always, associated with clockwise and anticlockwise precession of the magnetic vector respectively, when viewed from tail to tip (see Section 2.4). The first three bands are generally attributed to nondipole field effects, and the last to the dipole field. Since many of the records are not much longer than 10000–15000 yr, periods in the range of 5000–8000 yr are poorly defined and are strongly dependent on the type of detrend applied (Courtillot *et al.* 1977).

We have little information about periods greater than 10^4 yr. Kent and Opdyke (1977) noted a 43000 yr period in normalized intensity (NRM/ARM) in core RC10-167 from the NE Pacific, and in cores from the central Pacific, KH73-4-7, and SW Indian Ocean, RC14-14, Okubo and Takeuchi (1979) detected periods of 25000 and 18000 yr in normalized intensity (NRM/saturation IRM), but no clearly resolved periodicities in declination or inclination. The conflict between these two results is unresolved, but in neither study are the nominated spectral peaks very strong. An interesting feature of Okubo and Takeuchi's study is their modelling of the average trend in NRM spectra in terms of the output of the effective low pass filter caused by gradual acquisition of remanance within a finite zone of sediment. The required depth of partial magnetization came to the plausible figure of 10 cm.

There is a strong need to improve the quality of chronologies, and to address the question of uncertainty limits. Standard confidence limits for Fourier spectra (e.g. Bendat and Piersol, 1971) depend only on the instrinsic properties of the time series analysed. A detailed study of sets of cores from three lakes in SE Australia, each with independent radiocarbon chronologies (Barton and McElhinny, 1982) showed that the dominant source of error is inter-site variability between records. Careful

attention should be paid to calibration of radiocarbon time scales since this can result in shifts in periodicity of up to 25%.

2.3. INDENTIFICATION OF CAUSAL RELATIONSHIPS

Common periodicities in the spectra of different phenomena may be used to infer some direct or indirect causal relationship between them. In the field of geomagnetism the concept has been used to demonstrate a relationship between field fluctuations and the solar cycle (Currie, 1973; Courtillot and Le Mouel, 1976; Alldredge, 1976, 1977), the length of day (Jin and Thomas, 1977), and variations in varve thickness which must be climatically controlled (Ernesto and Pacca, 1981). Kent and Opdyke (1977) and Okubo and Takeuchi (1979) relate their 43000 and 25000 yr periodicities in normalized intensity to the 41000 yr period in obliquity and the 25800 yr period in precession of the Earth respectively. Unfortunately, both NRM/ARM and NRM/SIRM ratios may still contain a climatic signal (controlling the quantity and character of the magnetic mineral content) as well as a palaeointensity signal. Thus a simple correspondence of periodicities is not conclusive evidence for a link with geomagnetism.

2.4. ANALYSIS OF BAUER DIAGRAMS

Bauer (1895) observed that plots of declination vs inclination at different sites around the globe generally display clockwise looping. The pattern is particularly well developed at London and Paris though there are large regions of the globe where clockwise looping is not observed (Thompson, 1982). Runcorn (1959) demonstrated that for most plausible ranges of the spherical harmonic coefficients of the field, clockwise looping is a natural consequence of westward drift of the nondipole field, or westward precession of the main dipole. Skiles (1970) extended the argument for westward drifting radial dipoles situated in the outer regions of the core. Recently Dodson (1979) has drawn attention to the non-uniqueness of the clockwise looping/westward drift interpretation, but nevertheless 'Runcorn's Rule' is still applicable for a wide range of field configurations.

Bauer diagrams and virtual geomagnetic pole (VGP) paths covering large time intervals become complicated and are difficult to interpret. Spectral analysis of the vector time series expressed in terms of complex numbers (Denham, 1975), enables the sense, amplitude and ellepticity of looping to be determined as a function of frequency. Gonella (1972) defines a rotary coefficient, on a scale of -1 to $+1$, which provides a quantitative measure of the ellepticity and sense of looping ($+1$ = clockwise circular, -1 = anticlockwise circular). For the last 10000 yr or so, for which we have the semblance of world-wide coverage of data, no clear pattern of looping has yet emerged. There is, however, a noticeable tendency towards anticlockwise looping in the preferred long period band 5000–8000 yr, and clockwise

looping in the preferred band at 1000–3000 yr (see for example Oberg and Evans, 1977; Barton and McElhinny, 1982).

Should the underlying pattern of looping vary with time, results of conventional analysis in the frequency domain will be invalid, and time domain techniques should be used (e.g. Barton and McElhinny, 1981). Even if westward drift of nondipole sources continues uninterrupted, latitudinal drift of sources (Dodson, 1979) or interference patterns set up between oscillating sources (Creer and Tucholka, 1982) can result in a change in the sense of looping.

2.5. Modelling Source Configuration

In geomagnetism the three orthogonal components of the field are commonly treated independently, whereas for most palaeomagnetic secular variation work, vectors are assigned unit weights and reduced to declination and inclination series which again have usually been treated independently (e.g. Yukutake, 1962). This can be justified on the grounds that firstly it is possible for vertical and horizontal fluctuations of the field to be dominantly controlled by independent source mechanisms, and secondly our means of recovering and detecting vertical and horizontal signals are generally subject to different sources of uncertainty. The latter is particularly true of palaeomagnetic data obtained from cores of sediment: errors due to non-vertical corer penetration, twisting of the core tube during coring, inclination errors, current flow and bedding errors, and rotation of blocks of sediment within the core during transportation, subsampling and spinner measurement will not affect declinations and inclinations equally.

Wobble of a single dipole source will give secular variation records with similar declination and inclination spectra, whereas oscillations in moment of the dipole will only affect the scaling of the spectra. Although some sedimentary records show general agreement between the main periodicities in declination and inclination, for example the New England varve sequence (Johnson *et al.*, 1948, analysed by Yukutake, 1962), many exhibit a mismatch, e.g. Lake Windermere (Thompson, 1972) and Bessette Creek, British Columbia (Oberg and Evans, 1977). The effect is particularly prominent towards the low frequency ends of spectra where inclination peaks are commonly less numerous than declination peaks, and often have periods in the ratio of approximately 2:1 respectively (e.g. Oberg and Evans, 1977; Barton and McElhinny, 1982). Dating uncertainties, though affecting the overall form of the spectra, cannot account for these mismatches. Denham (1975) suggested that it might stem from the poor low frequency resolution of Fourier methods. However, the application of higher resolution (MEM) techniques to palaeomagnetic data (Oberg and Evans 1977; Turner and Thompson, 1981; Barton and McElhinny, 1982) indicates that the mismatch is real. Some insight into the cause for the mismatch is gained from the field perturbation at a point on the Earth's surface caused by a non-dipole source drifting beneath the site (Figure 7, Creer and Tucholka, 1982).

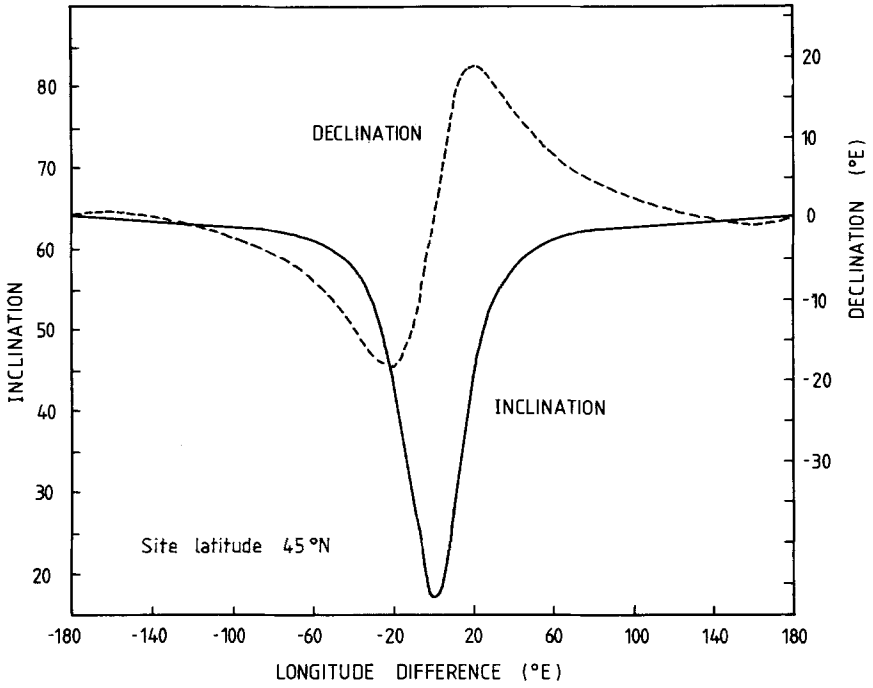

Fig. 7. Variation of declination and inclination caused by a radially outward pointing dipole of moment 0.075 × Earth's dipole moment situated at half the Earth's radius drifting westwards beneath a site at latitude 45° N. Internal attenuation is ignored.

During approximately equal time intervals the magnetic vector suffers a double deflection horizontally and a large single deflection vertically. *Short* record lengths containing such events would have spectra with the mismatch properties similar to those described in the previous paragraph. In practice the situation will be complicated by the presence of multiple non-dipole sources which grow and decay as well as drift. If the lifetime of some sources is short compared with the drift period, it is still feasible to get the above ~1:2 relationship between inclination and declination peaks for longer record lengths. An advantage of the spectral analysis approach to identifying source mechanisms is that even a limited knowledge of the relative shapes of the separate declination and inclination spectra is useful, and this is not sensitive to defects in time scales.

There is considerable scope for modelling source configurations (VGP paths) using the spectrum of complex equivalent palaeomagnetic directions (Section 4). In principle it should be possible to resolve the character of quite complex pole paths from the distribution of power in the complex number spectrum. Some examples are illustrated in Figure 8. The first corresponds to the quasi-hypotrochoidal dipole wobble hypothesized by Kawai and Hirooka (1967) which, if real, should appear as a common component in the spectrum of data from any site.

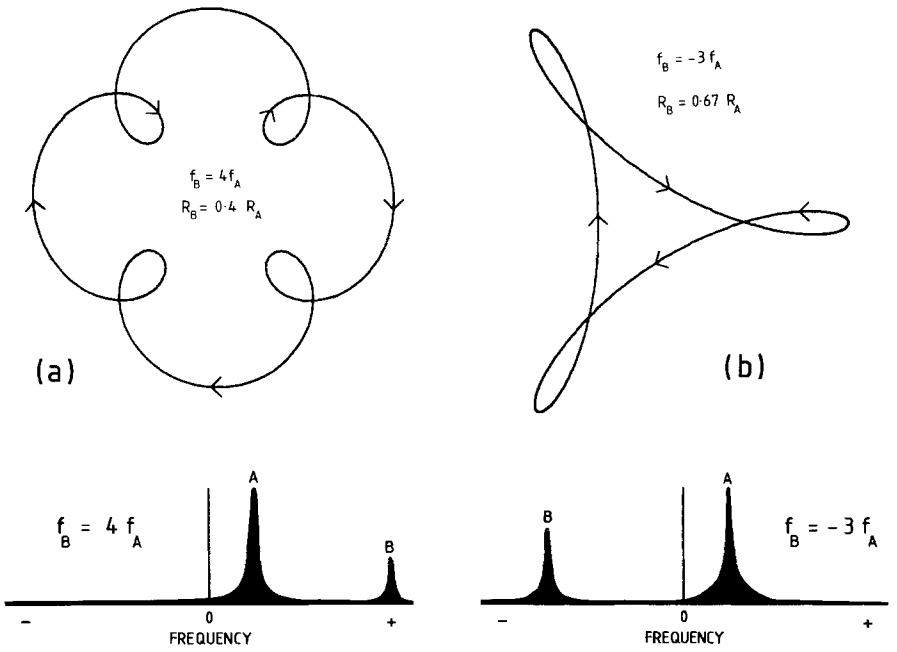

Fig. 8. Hypothetical complex number spectra of two vector paths in the complex plane. Each is the sum of two vectors of different lengths (R_a, R_b) rotating at different frequencies (f_a, f_b). Case (a) is analogous to Kawai and Hirooka's (1967) quasi-hypotrochoid.

The above applications are largely based on speculation. Analysis of synthetic secular variation records generated for a variety of physically plausible sources (and combinations thereof) is required to evaluate the technique.

2.6. GEOMAGNETIC POWER SPECTRUM

A satisfactory theory of the internal origin of the field must correctly predict the form of the continuous geomagnetic power spectrum. Based on observatory records, this has been well defined for periods between 1 and 100 yr (Currie, 1968; Allredge, 1977), but has been left to the realm of speculation for longer periods. Since palaeomagnetic records of the secular variation are generally directional only, the choice of time dependent variable is important.

Barton (1982) has made a preliminary synthesis of spectra for observatory, archaeomagnetic, lake sediment and marine sediment records (Figure 9). The spectral ordinate chosen was the sum of the power spectrum estimates for the Cartesian components (X, Y, Z) computed from declinations and inclinations assuming a total field strength corresponding to an axial geocentric dipole of present-day moment (8×10^{22} Am^2). The sum of spectral powers was smoothed and rescaled to get power spectral density estimates.

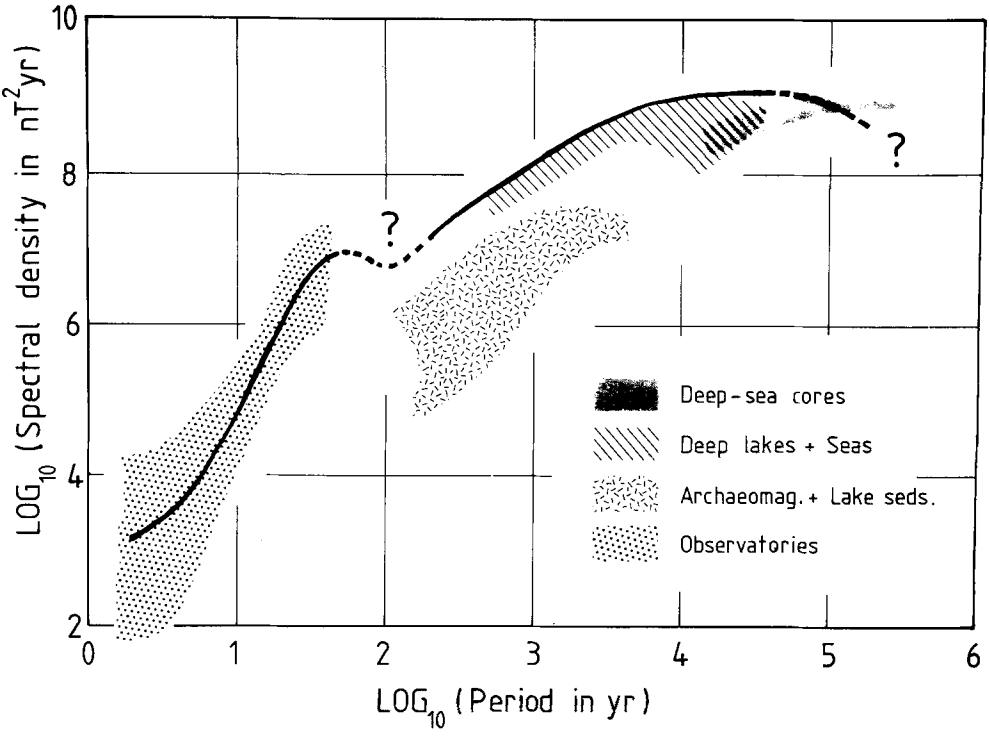

Fig. 9. A preliminary assessment of the continuous geomagnetic power spectrum derived from observatory and palaeomagnetic data. Individual spectra from the four classes of records fall within the shaded zones. Redrawn from Barton 1982. The solid line is a guess as to where the actual spectrum lies. Reasons why the lacustrine records underestimate the spectrum are discussed in the text and by Barton (1982).

Interpretation of the results must be made in the light of the following limitations: (i) the low frequency ends of spectra, particularly for observatory records, will be strongly dependent on the detrend applied (Courtillot *et al.*, 1977), (ii) the high frequency ends of spectra will underestimate the true spectrum due to loss of coherence of short period variations over long record lengths, and to attenuation (smoothing) of the geomagnetic signal by palaeomagnetic recording processes, and (iii) the deep-sea records are apparently dominated by noise. Bearing these in mind, the principle conclusions to be drawn are that no distinct boundary exists between the inferred frequency domains of dipole and nondipole field effects, the spectrum has a broad maximum between 10^4 and 10^5 yr, and there is the possibility of a dip at about 100 yr. If the latter is indeed the case, then a peak must occur in the region of 50 to 60 yr. A concentration of power in the geomagnetic spectrum at about 60 yr has been noted by many authors (e.g. Vestine and Kahle, 1968; Yukutake, 1973; Currie, 1973; Braginskiy and Fishman, 1977 and is attributed by Braginskiy to torsional oscillations in the magnetohydrodynamic dynamo (Braginskiy 1970a, b).

2.7. ANALYSIS OF THE MAGNETIC POLARITY TIME SCALE

Distribution functions which are useful for statistical modelling of the lengths of polarity intervals are discussed in Section 1.7 above. In order to reconcile the contrasting time scales of reversals ($\sim 10^6$ yr), dipole fluctuations ($\sim 10^4$ yr) and nondipole fluctuations (10^1–10^3 yr), Cox (1968) postulated that random fluctuations in the nondipole field combine with oscillations in the dipole field to trigger reversals. The probability of a reversal occuring during one cycle of dipole oscillation would have to be small and would be the same for all cycles. The problem amounts to assessing the probability of 'success' of a large number of trials, each with a low probability of success. A natural model to choose is therefore a Poisson process, which implies an exponential distribution of polarity intervals. Cox demonstrated that the lengths of polarity intervals are indeed plausible fits to exponential distributions with mean interval lengths of 0.18 My over 0–4.5 My, 0.23 My over 0–10.6 My, 0.33 My over 19.6-45 My, and 0.96 My over 45–75 My. Prior to 10.6 My an exponential curve only the data fits if we assume that a substantial number of short polarity intervals have not been detected. Nagata (1969) chose to interpret the physical model in terms of successive collapses of the geomagnetic field caused by the onset of symmetry in fluid motions in the core. The probability of regenerating a stable field thereafter would be the same for either polarity.

Naidu (1971) showed that a gamma process provides a better model than a Poisson process for the Hiertzler *et al.* (1968) polarity time scale from 0–76 My. Subsequently he concluded that polarity intervals are governed by a Markov model (Naidu, 1974) which implies that the core retains a memory of previous intervals. This has been disputed by Phillips, Blakely and Cox (1975) and Laj *et al.* (1979) who demonstrated that successive intervals are statistically independent – i.e. the generation process is a renewal process. Phillips (1977) found that both the gamma index (k) and the mean interval length (μ) for the best fitting gamma distribution vary over geological time. Furthermore, there are significant differences between gamma indices for normal and reversed intervals. He coined the name alternating renewal process to describe this phenomenon. McElhinny (1979) has reviewed the work of Phillips and co-workers, and emphasizes that only long-term changes in morophology and conditions within the core can account for variations in the distributions of polarity intervals.

One problem with the above distribution analyses is the sensitivity of results to undetected short polarity intervals. Laj *et al.* (1979) pointed out that an analysis using autocorrelation functions is less subject to this limitation. They concluded that successive polarity intervals are statistically independent, and are distributed in time according to a Poisson process. (The Poisson process is the special case of a gamma process when $k = 1$. As k increases the gamma distribution peaks away from the origin and tends to a Gaussian distribution. The spread of the distribution increases as k increases).

Spectrum analysis of the polarity time scale was first performed by Naidu (1971)

using ensemble averages of Fourier transforms. He reported a periodicity of 1.33 My in the Hiertzler *et al.* (1968) time scale (0–48 My), but subsequently Phillips and Cox (1976) failed to detect any spectral peaks in the same series from 0 to 45 My that were significantly different from the theoretical spectrum of a gamma process ($k = 1.55$, $\mu = 0.33$ My) at the 95% confidence level. This is consistent with the argument that polarity intervals are independent.

What emerges clearly from the above studies is that polarity intervals are independent and that parameters governing their distribution vary with time. In particular there is a sharp change in mean interval length at about 45 My. Prior to the Jurassic our knowledge of the polarity time scale is too incomplete to permit analyses of the above type. However, it is possible to estimate both the average polarity bias (percentage of time in normal or reversed polarity) and the average frequency of reversals over the whole of geologic time (Simpson, 1966; McElhinny, 1971; Creer, 1975; Irving and Pullaiah, 1976; review by McElhinny, 1979). Both variables display clearly defined large amplitude, long wavelength oscillations.

Maximum entropy analysis of polarity bias data for the Phanerozoic (Irving and Pullaiah), 1976) indicates periods of 300, 113, and 57 My. Most of the variance is accounted for by the former, and all peaks are relatively insensitive to sampling and averaging intervals. Earlier analyses of small data sets showed periods of 700 ± 100 My and 250 ± 50 My (Ulrych, 1972; maximum entropy analysis of McElhinny's, 1971 data), 350 My (McElhinny, 1971, nonquantitative assessment), and 300 ± 40 My and 80 ± 10 My (Crain *et al.*, 1969). The latter suggest possible relations with the 280 My period of rotation of the Milky Way and the 84 My period of vibration of the Sun normal to the galactic plane. The evidence for a period of about 300 My is strong. Both Irving and Pullaiah (1976) and McElhinny (1979) point out the correlation between these slow fluctuations in polarity bias and the long-term geological record as demonstrative of coupling between core and upper mantle processes.

3. Conclusion

Spectral analysis of palaeomagnetic data as independent declination and inclination series and as a series of complex equivalent directions (Denham, 1975) is valuable not only for detecting periodic characteristics of the geomagnetic secular variation, but also for describing and distinguishing between possible dipole and non-dipole source mechanisms. In particular, a more complicated declination spectrum with peaks at higher frequences than in the inclination spectrum is a consequence of a nondipole field caused by drifting radial dipole (or current loop) sources. Useful information can be obtained from the general forms of the spectra even if a precise time scale is not available.

Current evidence suggests that there are no discrete periodicities in the secular variation which can be traced world-wide, although there are loosely defined 'preferred' frequency bands: 60–70, 400-600, 1000–3000 and 5000–8000 yr. Very

long periods (43000, 25000, and 18000 yr) have been detected in NRM/ARM and NRM/SIRM ratios from deep-sea cores (Kent and Opdyke, 1977; Okubo and Takeuchi, 1979). However, it is far from certain that such periods can be attributed to variations in field strength.

There does not appear to be an abrupt change in the geomagnetic spectrum between the supposed frequency domains of nondipole and dipole effects. Indeed, since the nondipole-dipole division of the geomagnetic field is little more than a mathematical convenience, there is no reason why there should be. The often-presented argument about the contrast between characteristic times of non-dipole and dipole field fluctuation provides inadequate justification: since the dipole field is a spatial average, its fluctuations inevitably involve greater time-averaging (i.e. smoothing) than those in the non-dipole field.

The case for the independence of successive polarity intervals is strong. As increasing numbers of short polarity intervals are discovered it will be interesting to see whether the gamma indices of best fitting distributions approach unity (corresponding to a Poisson process). A more important issue is raised by Phillips' (1977) conclusion that the parameters describing the distribution of normal and reversed intervals are not the same. The implication that the geodynamo is not symmetric with respect to polarity state is profound.

Acknowledgements

Support for this work came from NERC grant GR3/3552 while the author was at the Geophysics Department, University of Edingburgh, and from NSF Grant EAR 850–1577.

Appendix: FORTRAN subroutines for MEM ANALYSIS

```
      SUBROUTINE SMYLIE (N,Z,LG,NF,FREQ,STEP,S)
C*************************************************
C SUBROUTINE TO COMPUTE THE MAXIMUM ENTROPY
C SPECTRUM FOR COMPLEX DATA USING THE
C ALGORITHM IN SMYLIE ET AL. (1973)
C Z    = COMPLEX DATA
C F    = FORWARD FILTER
C B    = BACKWARD FILTER
C N    = LENGTH OF Z
C G    = PREDICTION ERROR FILTER COEFFICIENTS
C LG   = NUMBER OF PREDICTION ERROR COEFICIENTS
C        (HENCE FILTER LENGTH = LG+1)
C FREQ= FREQUENCY SCALE
C NF   = LENGTH OF FREQ.
C*************************************************
      DIMENSION FREQ(NF),S(NF),P(64)
      COMPLEX Z(N),F(800),B(800),FF(800),G(64)
      COMPLEX CNOM,ARG,SUM
      DATA PI/3.141593/
```

```
C
C INITIALISE PARAMETERS:
C
      DO 5 I=1,N
      F(I)=Z(I)
5     B(I)=Z(I)
      KK=LG-1
      DO 10 I=1,KK
10    G(I)=CMPLX(0.0,0.0)
      P0=0.0
      DO 15 I=1,N
15    P0=P0+CABS(Z(I))**2
      P(1)=P0/FLOAT(N)
C
C START THE RECURSION,
C UPDATE THE FORWARD PREDICTION ERROR:
C
      DO 50 K=1,KK
      IF (K.EQ.1) GO TO 30
      DO 20 J=K,N
      FF(J)=F(J)
20    F(J)=F(J)+G(K-1)*B(J-K+1)
C
C UPDATE THE BACKWARD PREDICTION ERROR
C
      JJ=N-K+1
      DO 25 J=1,JJ
25    B(J)=B(J)+CONJG(G(K-1))*FF(J+K-1)
C
C UPDATE THE LAST FILTER COEFFICIENT:
C
30    CNOM=CMPLX(0.0,0.0)
      DEN=0.0
      JJ=N-K
      DO 35 J=1,JJ
      CNOM=CNOM+F(J+K)*CONJG(B(J))
35    DEN=DEN+CABS(F(J+K))**2+CABS(B(J))**2
      G(K)=-2.0/DEN*CNOM
C
C FIND THE REMAINING FILTER COEFFICIENTS,
C AND UPDATE THE ERROR POWER:
C
      IF(K.EQ.1) GO TO 47
      JJ=K-1
      DO 45 J=1,JJ
45    G(J)=G(J)+G(K)*CONJG(G(K-J))
47    P(K+1)=P(K)*(1.0-CABS(G(K))**2)
50    CONTINUE
C
C COMPUTE THE SPECTRUM, S(I) :
C
      ALPHA=-2.0*PI*STEP
      DO 65 I=1,NF
      SUM=CMPLX(0.0,0.0)
      DO 60 J=1,KK
      ZIM=ALPHA*FREQ(I)*FLOAT(J)
      ARG=CMPLX(0.0,ZIM)
60    SUM=SUM+G(J)*CEXP(ARG)
      DEN=CABS(1.0+SUM)**2
65    S(I)=P(LG)*STEP/DEN
      RETURN
      END
C-----------------------------------------
```

```
      SUBROUTINE ANDS (N,X,LG,G,PMX)
C*****************************************************
C MAXIMUM ENTROPY METHOD OF FOR SPECTRAL ANALYSIS
C SUGGESTED BY BURG (1967).
C X(N) = THE TIME SERIES OF LENGTH N
C LG = NUMBER OF PREDICTION ERROR COEFFICIENTS (MX+1)
C P(MX) = THE UPDATED VARIANCE
C A(MX) = THE 'ALPHA' PREDICTION ERROR COEFFICIENTS
C G(LG) = THE 'GAMMA' PREDICTION ERROR COEFFICIENTS
C MODIFIED ALGORITHM FROM N. ANDERSEN, (1974),
C GEOPHYSICS, VOL. 39, NO. 1,P. 69-72.
C ORIGINAL FORM OF PROGRAM WRITTEN BY J. R. CLEMENTS
C*****************************************************
      DIMENSION X(N),B1(800),B2(800),A(128),AA(128),
     +P(128),G(LG)
      PP=0.0
      MX=LG-1
C
C COMPUTE THE ARRAY OF PREDICTION ERROR COEFFICIENTS
C AND VARIANCES FOR M=1,MX
C
      DO 5 I=1,N
5     PP=PP+X(I)*X(I)
C
      P0=PP/FLOAT(N)
      M=1
      B1(1)=X(1)
      B2(N-1)=X(N)
      L=N-1
      DO 10 I=2,L
      B1(I)=X(I)
10    B2(I-1)=X(I)
      IF (M.EQ.1) GO TO 30
C
15    M=M+1
      LL=M-1
      DO 20 I=1,LL
      AA(I)=A(I)
20    CONTINUE
      LL=N-M
      DO 25 I=1,LL
      B1(I)=B1(I)-AA(M-1)*B2(I)
25    B2(I)=B2(I+1)-AA(M-1)*B1(I+1)
C
30    XNOM=0.0
      DEN=0.0
      LL=N-M
      DO 35 I=1,LL
      XNOM=XNOM+B1(I)*B2(I)
35    DEN=DEN+B1(I)*B1(I)+B2(I)*B2(I)
C
      A(M)=2.0*XNOM/DEN
      IF(M.EQ.1)POM=P0
      IF(M.NE.1)POM=P(M-1)
      P(M)=POM*(1.0-A(M)*A(M))
      IF (MX.EQ.1) GO TO 45
      IF (M.EQ.1) GO TO 15
      LL=M-1
      DO 40 I=1,LL
40    A(I)=AA(I)-A(M)*AA(M-I)
45    IF (M.NE.MX) GO TO 15
      IF(MX.EQ.1)PMX=P0
      IF(MX.NE.1)PMX=P(MX)
C
      WRITE (6,60) PMX
60    FORMAT (' UPDATED VARIANCE =',F14.4)
      G(1)=1.0
      DO 50 I=2,LG
50    G(I)=-A(I-1)
      DO 55 I=1,MX
55    P(LG+1-I)=P(LG-I)
      P(1)=P0
      RETURN
      END
```

```
      SUBROUTINE SPECT (LG,G,NF,FREQ,PLG,STEP,S)
C**********************************************
C SUBROUTINE TO COMPUTE THE MAXIMUM ENTROPY
C SPECTRAL DENSITY FUNCTION (S) FROM THE REAL
C PREDICTION ERROR COEFFICIENTS G(LG).
C THE FILTER LENGTH IS LG+1
C**********************************************
      DIMENSION G(LG),S(NF),FREQ(NF)
      COMPLEX SUM,ARG
      DATA PI/3.14159/
C
      ALPHA=-2.0*PI*STEP
      DO 55 I=1,NF
      SUM=CMPLX(0.0,0.0)
      DO 50 K=1,LG
      XIMAG=ALPHA*FREQ(I)*FLOAT(K-1)
      ARG=CMPLX(0.0,XIMAG)
50    SUM=SUM+G(K)*CEXP(ARG)
C
      DEN=CABS(SUM)**2
      S(I)=(PLG*STEP)/DEN
55    CONTINUE
      RETURN
      END
C
```

References

Akaike, H.: 1969a, 'Fitting Autoregressive Models for Prediction', *Ann. Inst. Statist. Math.* **21**, 243–247.

Akaike, H.: 1969b, 'Power Spectrum Estimation through Autoregressive Model Fitting', *Ann. Inst. Statist. Math.* **21**, 407–419.

Akaike, H.: 1970, 'Statistical Predictor Identification', *Ann Inst. Statist. Math.* **22**, 203–217.

Akaike, H.: 1974, 'A New Look at the Statistical Model Identification', *IEEE Trans. Automat. Control*, AC**19**, 716–723.

Akaike, H.: 1976, 'Canonical Correlation Analysis of Time Series and the Use of an Information Criterion, in R. K. Mehra and D. G. Lainiotis (eds.), *System Identification – Advances and Case Studies*, Academic Press, New York, p. 27–96.

Alldredge, L. R.: 1976, 'Effects of Solar Activity on Annual Means of Geomagnetic Components', *J. Geophys. Res.* **81**, 2990–2996.

Alldredge, L. R.: 1977, 'Geomagnetic Variations with Periods from 13 to 30 years, *J. Geomag. Geoelectr.* **29**, 123–135.

Andersen, N.: 1974, 'On the Calculation of Filter Coefficients for Maximum Entropy Spectral Analysis', *Geophysics*, **39**, 69–72.

Bartlett, M. S.: 1948, 'Smoothing Periodograms from Time Series with Continuous Spectra', *Nature* **161**, 686–687.

Barton, C. E.: 'Spectral Analysis of Palaeomagnetic Times Series and the Geomagnetic Spectrum', *Phil. Trans. Roy. Soc. A* (in press).

Barton, C. E. and McElhinny M. W.: 1981, 'A 10000 yr Geomagnetic Secular Variation Record from Three Australian Maars', *Geophys. J. Roy. Astr. Soc.*, **67**, 465–485.

Barton, C. E. and McElhinny, M. W.: 1982, 'Time Series Analysis of the 10000 yr Geomagnetic Secular Variation Record from SE Australia', *Geophys. J. Roy. Astr. Soc.* **68**, 709–724.

Barton, C. E., Merrill, R. T., and Barbetti, M.: 1979, 'Intensity of the Earth's Magnetic Field over the Last 10000 Years', *Phys. Earth Planet. Int.* **20**, 96–110.

Bauer, L. A.: 1895, 'On the Secular Motion of a Free Magnetic Needle, II', *Rev. Phys.* **3**, 34–48.

Bendat, J. S. and Piersol, A. G.: 1971, *Random Data: Analysis and Measurement Procedures*, John Wiley, NY, pp. 407.

Berkhout, A. J. and Zaanen, P. R.: 1976, 'A Comparison between Wiener Filtering, Kalman Filtering, and Deterministic Least Squares Estimation', *Geophy. Prospecting* **24**, 141–197.

Berryman, J. G.: 1978, 'Choice of Operator Length for Maximum Entropy Spectral Analysis', *Geophysics* **43**, 1384–1391.

Blackman, R. B. and Tukey, J. W.: 1959, *The Measurement of Power Spectra, from the Point of View of Communications Engineering*, Dover, New York.

Bloomfield, P.: 1976, *Fourier Analysis of Time Series: An Introduction*, John Wiley, New York, pp. 258.

Box, G. E. P. and Jenkins, G. M.: 1970, *Time Series Analysis, Forecasting and Control,* Holden-Day, San Francisco (Revised ed., 1976).
Braginskiy, S. I.: 1970a, 'Torsional Magnetohydrodynamic Vibrations in the Earth's Core and Variations in Day Length', *Geomagn. Aeron.* **10**, 1–8.
Braginsky, S. I.: 1970b, 'Oscillation Spectrum of the Hydromagnetic Dynamo of the Earth', *Geomag. Aeron.* **10**, 172–181.
Braginskiy, S. I. and Fishman, V. M.: 1977, '60-yr Variations of the Geomagnetic Field and of the Electrical Conductivity of the Mantle', *Geomag. Aeron.* **17**, 607–613.
Brillinger, D. R.: 1973, 'An Empirical Investigation of the Chandler Wobble and Two Proposed Excitation Processes', *Bull. Int. Stat. Inst.* **45**, 413–434.
Bucha, V.: 1967: 'Intensity of the Earth's Magnetic Field During Archaeological Times in Czechoslovakia', *Archaeometry* **10**, 12–22.
Bucha, V.: 1969, 'Changes of the Earth's Magnetic Moment and Radiocarbon Dating', *Nature* **224**, 681–683.
Bullard, E. C., Freedman, C., Gellman, H., and Nixon, J.: 1950, 'The Westward Drift of the Earth's Magnetic Field', *Phil. Trans. Roy. Soc. Lond. A,* **243**, 67–92.
Burg, J. P.: 1967, 'Maximum Entropy Spectral Analysis', *37th Ann. Int. Meeting Soc. Explor. Geophys.,* Oklahoma City, 1967, (see also Burg, Ph.D. Thesis, 1975).
Burg, J. P.: 1968, 'A New Analysis for Time Series Data', *Adv. Study Inst. on Signal Processing,* NATO, Enschede (see also Burg, Ph.D. Thesis, 1975).
Chatfield, C.: 1980, *The Analysis of Time Series: An Introduction,* Chapman and Hall, London, 2nd edition, pp. 268.
Chen, W. Y. and Stegen, G. R.: 1974, 'Experiments with Maximum Entropy Power Spectra of Sinusoids', *J. Geophys. Res.* **79**, 3019–3022.
Claerbout, J. F.: 1976, *Fundamentals of Geophysical Data Processing,* McGraw Hill, New York, pp. 274.
Claerbout, J. F. and Muir, F.: 1973, 'Robust Modelling with Erratic Data', *Geophysics* **38**, 826–844.
Clark, R. M.: 1975, 'A Calibration Curve for Radiocarbon Dates, *Antiquity* **49**, 251–266 (and comments by Suess and reply, *Antiquity* **50**, 61–63).
Clark, R. M. and Thompson, R.: 1978, 'An Objective Method for Smoothing Palaeomagnetic Data', *Geophys. J. Roy. Astr. Soc.* **52**, 205–213.
Cooley, J. W. and Tukey, J. W.: 1965, 'An Algorithm for the Machine Calculation of Complex Fourier Series' *Math. Comp.* **19**, 297–301.
Courtillot, V. E. and Le Mouël, J. L.: 1976, 'On the Long Period Variations of the Earth's Magnetic Field from 2 Months to 20 Years', *J. Geophys. Res.* **81**, 2941–2950.
Courtillot, V., Le Mouël, J. L., and Mayaud, P. N.: 1977, 'Maximum Entropy Spectrum Analysis of the Geomagnetic Activity Index aa over a 107-yr Interval', *J. Geophys. Res.* **82**, 2641–2649.
Cox, A.: 1968, 'Lengths of Geomagnetic Polarity Intervals', *J. Geophys. Res.* **73**, 3247–3260.
Cox, A.: 1969, 'Geomagnetic Reversals', *Science* **163**, 237–245.
Cox, D. R.: 1962, *Renewal Theory,* Methuen, London.
Cox, D. R. and Lewis, P. A. W.: 1966, *The Statistical Analysis of Series of Events,* Methuen, London.
Cox, D. R. and Miller, H. D.: 1965, *The Theory of Stochastic Processes,* John Wiley, N.Y.
Crain, I. K., Crain, P. L., and Plaut, M. G.: 1969, 'Long Period Fourier Spectrum of Geomagnetic Reversals', *Nature* **223**, 283.
Creer, K. M.: 1975, 'On a Tentative Correlation between Changes in Geomagnetic Polarity Bias and Reversal Frequency and the Earth's Rotation, through Phanerozoic Time', in *'Growth Rhythms and the History of the Earth's Rotation, ed.* G. D. Rosenberg and S. K. Runcorn (eds.), John Wiley & Sons, London, pp. 293–318.
Creer, K. M., Thompson, R., Molyneux, L., and Mackereth, F. J. H.: 1972, 'Geomagnetic Secular Variation Recorded in the Stable Magnetic Remanence of Recent Sediments', *Earth Planet. Sci. Letters* **14**, 115–127.
Creer K. M., and Tucholka, P.: 1982, 'Secular Variation as Recorded in Lake Sediments: A Discussion of North American and European Results', *Phil. Trans. Roy. Soc. (in press).*
Currie, R. G.: 1968, 'Geomagnetic Spectrum of Internal Origin and Lower Mantle Conductivity', *J. Geophys. Res.* **73**, 2779–2786.
Currie, R. G.: 1973, *'Geomagnetic Line Spectra* – 2 to 70 Years', *Astrophys. Space Sci.* **21**, 425–438.
Daniell, P. J.: 1946, 'Discussion on the Symposium on Autocorrelation in Time Series', *J. Roy. Stat. Soc.* (Suppl.) **8**, 88–90.

Davis, J. C.: 1973, *Statistics and Data analysis in Geology*, John Wiley, New York, pp. 550.
De Boor, C.: 1978, *A practical Guide to Splines*, Springer-Verlag, NY.
De Boor, C.: 1980, 'FFT as Nested Multiplication, with a Twist', *SIAM, J. Sci. Stat. Comput.* **1**, 173–178.
Deeming, T. J.: 1975, 'Fourier Analysis with Unequally Spaced Data', *Astrophys. Space Sci.* **36**, 137–158.
Denham, C. R.: 1975, 'Spectral Analysis of Paleomagnetic Time Series', *J. Geophys. Res.* **80**, 1897–1901.
Dodson, R. E.: 1979, 'Counterclockwise Precession of the Geomagnetic field Vector and Westward Drift of the Non-dipole Field', *J. Geophys. Res.* **84**, 637–644.
Ernesto, M. and Pacca, I. G.: 1981, 'Spectral Analysis of Permocarboniferous Geomagnetic Variation Data from Glacial Rhythmites', *Geophys. J. Roy. Astr. Soc.* **67**, 641–647.
Fougere, P. F., Zawalick, E. J., and Radoski, H. R.: 1976, 'Spontaneous Line Splitting in Maximum Entropy Power Spectrum Analysis', *Phys. Earth Planet. Int.* **2**, 201–207.
Gonella, J.: 1972, 'A Rotary Component Method for Analysing Meteorological and Oceanographic Vector Time Series' *Deep Sea Res.* **19**, 833–846.
Haykin, S.: 1979, *Non Linear Methods of Spectral Analysis* Springer-Verlag, Berlin.
Hiertzler, J. R., Dickson, G. O., Herron, E. M., Pitman, W. C., III, and Le Pichon, X.: 1968, 'Marine Magnetic Anomalies, Geomagnetic Field Reversals, and Motions of the Ocean Floor and Continents', *J. Geophys. Res.*, **73**, 2119–2136.
Irving, E. and Pullaiah, G.: 1976, 'Reversals of the Geomagnetic Field, Magnetostratigraphy, and Relative Magnitude of Paleosecular Variation in the Phanerozoic', *Earth Sci. Rev.* **12**, 35–64.
Jenkins, G. M. and Watts, D. G.: 1968, *Spectral Analysis and Its Applications,* Holden-Day, San Francisco.
Jin, Rong-Sheng and Thomas, D. M.: 1977, 'Spectral Line Similarity in the Geomagnetic Dipole Field Variations and Length of Day Fluctuations', *J. Geophys. Res.* **82**, 828–834.
Johnson, E. A., Murphy, T., and Torreson, O. W.: 1948, 'Prehistory of the Earth's Magnetic Field', *Terr. Magn. Atmos. Electr.* **53**, 349–372.
Jones, R. H.: 1965, 'A Reappraisal of the Periodogram in Spectral Analysis', *Technometrics* **7**, 531–542.
Kanasewich, E. R.: 1975, *Time Sequences Analysis in Geophysics,* University of Alberta Press, Edmonton, pp. 364.
Kane, R. P.: 1977, 'Power Spectrum Analysis of Solar and Geophysical Parameters', *J. Geomag. Geoelectr.* **29**, 471–495.
Kawai, N. and Hirooka, K.: 1967, 'Wobbling Motion of the Geomagnetic Dipole Field in Historic Time During these 2000 Years. *J. Geomag. Geoelectr.* **19**, 217–227.
Kedem, B.: 1980, *Binary Time Series,* Marcel Dekker, NY.
Kent, D. V. and Opdyke, N. D.: 1977, 'Palaeomagnetic Field Intensity Variation Recorded in a Brunhes Epoch Deep-Sea Sediment Core, *Nature* **266**, 156–159.
Koopmans, L. H.: 1974, *The Spectral Analysis of Time Series*, Academic Press, New York.
Lacosse, R. T.: 1971, 'Data Adaptive Spectral Analysis Methods', *Geophysics* **36**, 661–675.
Laj, C., Nordemann, D., and Pomeau, Y.: 1979, 'Correlation Function Analysis of Geomagnetic Field Reversals', *J. Geophys. Res.* **84**, 4511–4515.
Lee, Y. W.: 1960, *Statistical Theory of Communication,* John Wiley, NY.
McElhinny, M. W.: 1971, 'Geomagnetic Reversals During the Phanerozoic', *Science* **172**, 157–159.
McElhinny, M. W.: 1979, 'Palaeogeomagnetism and the Core-Mantle Interface', in M. W. McElhinny (ed.), *The Earth: Its Origin, Structure and Evolution*, Academic Press, London, 113–136.
McGee, T. M.: 1969, *On Burg's Method of Spectral Analysis,* Unpublished Manuscript, Vening Meinesz Laboratory, Utrecht.
Mackereth, F. J. H.: 1971, 'On the Variation in Direction of the Horizontal Component of Remanent Magnetization in Lake Sediments', *Earth Planet. Sci. Letters* **12**, 332–338.
McNeil, D. R., 1977, *Interactive Data Analysis*, Wiley and Sons, New York, pp. 186.
Nagata, T.: 1969, 'Length of Geomagnetic Polarity Intervals', *J. Geomag. Geoelectr.* **21**, 701–704.
Naidu, P. S.: 1971, 'Statistical Structure of Geomagnetic Field Reversals', *J. Geophys. Res.* **76**, 2649–2662.
Naidu, P. S.: 1974, 'Are Geomagnetic Reversals Independent?', *J. Geomag. Geoelectr.* **26**, 101–104.
Oberg, C. J. and Evans, M. E., 'Spectral Analysis of Quaternary Palaeomagnetic Data from British Columbia and its bearing on Geomagnetic Secular Variation', *Geophys. J. Roy. Astr. Soc.* **51**, 691–699.

Okubo, S. and Takeuchi, H.: 1979, 'Time Series Analysis of Natural Remanent Magnetization in Deep-Sea Sediments', *Geophys. J. Roy. Astr. Soc.* **56**, 309–318.
Phillips, J. D.: 1977, 'Time Variation and Asymmetry in the Statistics of Geomagnetic Reversal Sequences', *J. Geophys. Res.* **82**, 835–843.
Phillips, J. D. and Cox, A.: 1976, 'Spectral Analysis of Geomagnetic Reversal Time Scales', *Geophys. J. Roy. Astr. Soc.* **45**, 19–33.
Phillips, J. D., Blakely, R. J. and Cox, A.: 'Independence of Geomagnetic Polarity Intervals', *Geophys. J. Roy. Astr. Soc.* **43**, 747–754.
Pisarenko, V. F.: 1972, 'On the Estimation of Spectra by Means of Non-Linear Functions of the Covariance Matrix', *Geophys. J. Roy. Astr. Soc.* **28**, 511–531.
Runcorn, S. K.: 1959, 'On the Theory of the Geomagnetic Secular Variation', *Ann. de Geophys.* **15**, 87–92.
Schuster, A.: 1898, 'On the Investigation of Hidden Periodicities with Application to a supposed 26 Day Period of Meteorological Phenomena', *Terr. Magn.* **3**, 13–41.
Simpson, J. F.: 1966, 'Evolutionary Pulsations and Geomagnetic Polarity', *Bull. Geol. Soc. Amer.* **77**, 197–203.
Singleton R. C.: 1968, 'Algorithm 339. An ALGOL Procedure for the fast Fourier Transform with Arbitrary Factors (C6)', *Communications of the ACM* **11**, 776–782.
Skiles, D. D.: 1970, 'A method of Inferring the Direction of Drift of the Geomagnetic Field from Paleomagnetic Data', *J. Geomag. Geoelectr.* **22**, 441–462.
Smylie, D. E., Clark, G. K. C., and Ulrych, T. J.: 1973, 'Analysis of Irregularities in the Earth's Rotation', In *Methods in Computational Physics*, **13**, 391–430, Academic Press, New York.
Stuiver, M.: 1978, 'Radiocarbon Timescale Tested Against Magnetic and Other Dating Methods', *Nature* **273**, 271–274.
Swingler, D. N.: 1979, 'A Comparison Between Burg's Maximum Entropy Method and a Non-Recursive Technique for the Spectral Analysis of Deterministic Signals', *J. Geophys. Res.* **84**, 679–685.
Swingler, D. N.: 1980, 'Burg's Maximum Entropy Algorithm Versus the Discrete Fourier Transform as a Frequency Estimator for Truncated Real Sinusoids', *J. Geophys. Res.* **85**, 1435–1438.
Thompson, R.: 1972, 'Magnetic Studies of Selected Sedimentary Sequences', Ph.D. Thesis, University of Newcastle.
Thompson, R.: 1982, 'A Comparison of Geomagnetic Field Behavior as Recorded by Historical, Archaeomagnetic and Palaeolimnological Data', *Phil. Trans. Roy. Soc. Lond.* **A.**, (in press).
Thompson, R. and Turner, G.M.: 1979, 'British Geomagnetic Master Curve 10000–0 yr B.P. for Dating European Sediments', *Geophys. Res. Letters*, **6**, 249–252.
Toman, K.: 1965, 'Spectral Shifts of Truncated Sinusoids', *J. Geophys. Res.* **70**, 1749–1750.
Treitel, S., Gutowski, P. R., and Robinson, E. A.: 1977, 'Empirical Spectral Analysis Revisited', In: *Topics in Numerical Analysis* **3**, Academic Press, New York.
Tukey, J. W.: 1977, *Exploratory Data Analysis*, Addison-Wesley, Massachusetts.
Turner, G. M. and Thompson, R.: 1981, 'Lake Sediment Record of the Geomagnetic Secular Variation Record in Britain During Holocene Times', *Geophys. J. Roy. Astr. Soc.* **65**, 703–725.
Ulrych, T. J.: 1972, 'Maximum Entropy Power Spectrum of Long Period Geomagnetic Reversals', *Nature* **235**, 218–219.
Ulrych, T. J. and Bishop, T. N. 1975, 'Maximum Entropy Spectral Analysis and Autoregressive Decomposition', *Rev. Geophys. Space Phys.* **13**, 183–200.
Ulrych, T. J. and Clayton, R. W.: 1976, 'Time Series Modelling and Maximum Entropy', *Phys. Earth Planet. Inter.* **12**, 188–200.
Yukutake, T.: 1962, 'The Westward Drift of the Magnetic Field of the Earth', *Bull. Earthquake Res. Inst. Tokyo* **40**, 1–65.
Yukutake, T.: 1973, 'Fluctuations in the Earth's Rate of Rotation Related to Changes in the Geomagnetic Dipole Field', *J. Geomag. Geoelectr.* **25**, 195–212.
Yule, G. U.: 1927, 'On a Method of Investigating Periodicities in Disturbed Series, with Special Reference to Wolfer's Sunspot Numbers', *Phil. Trans. Roy. Soc. London, Ser.* A **226**, 267–298.
Vestine, E. H. and Kahle, A. B.: 1968, 'The Westward Drift and Geomagnetic Secular Change', *Geophys. J. Roy. Astr. Soc.* **15**, 29–37.